*Molecular Vision* 2025; 31:69-83 <http://www.molvis.org/molvis/v31/69>
Received 18 November 2024 | Accepted 24 March 2025 | Published 26 March 2025



# Syndromic forms of inherited retinal dystrophies: a comprehensive molecular diagnosis of consanguineous Pakistani families using capture panel sequencing

**Aleesha Asghar,[1] Sumbal Wazir,[1] Shehzeen Fatima,[1] Hussan Bilal,[1] Muhammad Shoaib,[1] Saqib Ur Rehman,[1] Sumaira Altaf,[2] Yumei Li,[3] Kiran Afshan,[1] Rui Chen,[3] Sabika Firasat[1,4]**

*[1]Department of Zoology, Faculty of Biological Sciences, Quaid-i-Azam University, Islamabad, Pakistan; [2]Department of Pediatric Ophthalmology and Strabismus, Al-Shifa Trust Eye Hospital, Jhelum Road, Rawalpindi, Pakistan; [3]Department of Ophthalmology, Center for Translational Vision Research, University of California, Irvine School of Medicine, CA; [4]Department of Molecular and Human Genetics, Baylor College of Medicine, Houston, TX*

**Background:** Inherited retinal dystrophies (IRDs) represent a clinically and genetically heterogeneous group of genetic disorders that involve photoreceptors and/or retinal pigment epithelium degeneration. IRDs may occur as an isolated condition or may represent an ocular manifestation of a multisystemic disorder referred as syndromic IRD. To increase the understanding of the molecular determinants of syndromic IRD-related genes in the Pakistani population, we revealed the genetic profile of 13 consanguineous Pakistani families using capture panel sequencing.
**Methods:** We performed comprehensive molecular testing on 72 IRD segregating Pakistani families using targeted capture panel sequencing of 344 known genes. The pathogenicity of candidate variants was assessed using American College of Medical Genetics and Genomics guidelines, followed by Sanger sequencing for segregation analysis.
**Results:** Causative variants in previously reported syndromic IRDs genes were detected in 13/72 (18%) IRD families, including 5/72 (6.94%), 4/72 (5.55%), 2/72 (2.8%), 1/72(1.38%) and 1/72 (1.38%) in Usher syndrome, Bardet–Biedl syndrome, Batten disease, retinitis pigmentosa with situs inversus and Stickler syndrome segregated families, respectively. Disease-causing variants included nine previously reported and six novel homozygous variants, i.e., c.1143G>C in *USH2A*, c.470G>A in *MYO7A*, c.877–2A>G in *PCDH15*, c.347C>T in *ARL6*, c.581C>T in *CLN5* and c.100+1G>T in *ARL2BP* gene segregation with disease phenotype in eight families. Two heterozygous variants of the *USH2A* gene, i.e., c.12093C>A and c.9815C>T, were segregated in a compound heterozygous form in family RP243. Furthermore, RP151 showed segregation of a heterozygous variant c.247G>A in a Stickler syndrome gene, i.e., *COL2A1*, in an autosomal dominant manner.
**Conclusions:** This study reaffirms the clinical and genetic heterogeneity of syndromic IRD-associated genes and confirms the usefulness of molecular methods in advancing our understanding of these conditions in consanguineous populations. The most commonly mutated Bardet–Biedl syndrome gene was *ARL6* (75%) and the most commonly mutated Usher syndrome genes were *USH2A* (40%) and *MYO7A* (40%). Our data could serve as a reference for future studies and the development of treatment modalities for affected families of Pakistani origin.

Inherited retinal dystrophies (IRDs) are a group of genetic retinal dystrophies characterized by photoreceptor and retinal pigment epithelium abnormalities that lead to progressive retinal degeneration, atrophy and vision loss [1,2]. IRDs are subdivided into nonsyndromic IRDs, without systemic abnormalities, and syndromic IRDs, in which retinal degeneration is associated with other symptoms due to systemic diseases [2–4]. Syndromic IRDs are classified into four main categories, comprising ciliopathies, Usher syndrome, inborn errors of metabolism (IEMs) and mitochondrial disorders [4,5]. Management of syndromic IRD cases requires definitive diagnosis and a thorough understanding of these conditions.

Ciliopathies, which result from primary cilium dysfunction, often exhibit pleiotropic effects, causing abnormalities in the eyes as well as urinary, central nervous and skeletal systems [3,5]. Variants in protein-encoding genes related to ciliary structure or function are known to cause approximately 36% of genetically diagnosed cases of retinal degeneration [5]. Photoreceptors are modified primary cilia that are susceptible to ciliopathy-related dysfunction, leading to the retinitis pigmentosa (RP) phenotype, as observed in Bardet–Biedl syndrome (BBS), Senior-Løken syndrome and Alstrom syndrome [5–7]. BBS shows heterogeneous clinical manifestations encompassing primary features of the disease: rod–cone dystrophy, polydactyly, obesity, genital abnormalities, renal defects and learning difficulties, and secondary

Correspondence to: Sabika Firasat; Department of Zoology, Faculty of Biological Sciences, Quaid-i-Azam University, University Road, 45320, Islamabad, Pakistan. Phone: +9290644410. FAX: +9290643170; email: sabika.firasat@qau.edu.pk

features such as developmental delay, speech deficit, brachydactyly/syndactyly, dental defects, ataxia/poor coordination, olfactory deficit, diabetes mellitus, congenital heart disease, and so on [8]. However, most of these characteristics often appear and progressively get worse in the first and second decades of life [9]. To confirm the diagnosis of BBS, it is recommended that the patient bears four out of six primary features of the disease. If only three primary features are detected, two secondary features are required to confirm the BBS diagnosis. However, these criteria focus on BBS mostly as a clinical entity and ignore attenuated forms of the disease and the possible gene-specific manifestations [10,11].

In case of BBS, more than 20 genes (*BBS1*, *BBS2*, *ARL6*, *BBS4*, *BBS5*, *BBS6/MKKS*, *BBS7*, *TTC8*, *BBS9*, *BBS10*, *TRIM32*, *BBS12*, *MKS1*, *CEP290*, *WDPCP*, *SDCCAG8*, *LZTFL1*, *BBIP*, *IFT27*, *IFT74*, *C8orf37*, *SCLT1*, *NPHP1*, *SCAPER*) have already been identified [12–14]. BBS is a rare condition with differing frequencies among various geographic areas. It ranges between 1:120,000 and 1: 160,000 in North America and Europe. However, the rate is higher in some isolated areas where consanguineous marriages are common. For example, the prevalence rate is far higher among the mixed Arab population in Kuwait (1:36,000), among Bedouins (1:13,500), in the Jahra district (1:6900), in Newfoundland (1:18,000) and in the Faroe Islands (1:3700) [15].

Usher syndrome accounts for the most prevalent cause of deaf-blindness world, with a prevalence of 4–17 per 100,000 people. It causes simultaneous loss of vision and hearing with vestibular dysfunction in some cases [16]. It is inherited in an autosomal recessive manner [17]. Usher syndrome is primarily categorized into 3 clinical types: USH1, USH, and USH3, which are further subcategorized into 14 subtypes. Each subtype is caused by a mutation in a distinct gene. Nine specific genes have been discovered causing Usher syndrome, among which *MYO7A*, *USH1C*, *CDH23*, *PCDH15* and *USH1G* are associated with USH type 1; *USH2A*, *ADGR1* and *WHRN* contribute to USH type 2, and *CLRN1* contributes to USH type 3 [18]. USH-involved mutations disrupt structural proteins in the auditory, visual and vestibular systems. The impairment of sensory cells expressing actin filaments is seen to be constrained, explaining the impairment of eyes and ears in affected individuals [19].

In Usher syndrome, sensorineural hearing loss alongside progressive RP is evident. At the same time, the onset and severity of hearing loss, together with the presence of vestibular dysfunction, determine the type of syndrome. Within each subtype of Usher syndrome, vast clinical heterogeneity facilitates an atypical presentation [16]. The prevalence data for Usher syndrome is ambiguous with large differences observed internationally, probably due to the lack of proper diagnostic and rehabilitation facilities [18]. However, the global prevalence approximation lies at 1 in 30,000 individuals, and some alternate investigations have revealed the aforementioned wide occurrence range from 4 to 17 in every 100,000 people [16].

In IEMs, neurologic symptoms are common. As the retina develops from the embryonic forebrain thus, neurodegeneration resulting from IEMs often involves retinal degeneration. Many syndromic IRDs are as a result of IEMs, including neuronal ceroid lipofuscinoses (CLNs), and types 1 and 2 Stickler syndrome (SS) [4]. CLNs are autosomal recessive conditions caused by mutations in genes that lead to endo-lysosomal dysfunction. CLNs, also known as Batten disease, are neurodegenerative disorders with a common presentation of early vision impairment and progressive neuronal loss [20]. To date, mutations in at least 14 genes are known to cause CLN phenotypes [21]. SS is a subtype of collagenopathy that was initially named “hereditary progressive arthro-ophthalmopathy” by Gunnar B. Stickler, who first studied and reported the findings of this syndrome in 1965 [22]. SS can be inherited as an autosomal dominant condition due to heterozygous disease-causing variants in the *COL2A1*, *COL11A1* and *COL11A2* genes, or as an autosomal recessive condition due to biallelic variants in the *COL9A1*, *COL9A2* and *COL9A3* genes [23]. SS is a group of connective tissue disorders that is associated with short sight and a very high risk of blindness from retinal detachment. Other features include cleft palate, conductive or sensorineural hearing loss, orofacial anomalies and premature arthritis [24,25]. SS is clinically and genetically heterogeneous and shows variable expression; therefore, mild forms of the disease often remain unrecognized, necessitating the use of molecular genetic techniques in the diagnosis of suspected cases for patient management and identification of at-risk family members [26]. In an ongoing effort to study the spectrum and frequency of disease-causing variants in a large-scale Pakistani IRD cohort using next-generation sequencing techniques, we identified disease-causing variants in syndromic IRD genes in 13 families, explaining the clinical and genetic heterogeneity of these conditions.

## METHODS

*Ethical approval and enrollment of families:* Prior approval for the research presented here was obtained from the Bio-Ethical Review Committee of the Faculty of Biologic Sciences, Quaid-i-Azam University Islamabad, Pakistan. Ophthalmologists from Al-Shifa Trust Eye Hospital in

Rawalpindi, Pakistan conducted a clinical assessment of all enrolled families and confirmed a diagnosis of retinal phenotype in each family. Clinical assessments for the retinal dystrophy phenotype included a detailed family and medical history, physical examination, fundoscopy, slit lamp examination and visual acuity testing. Furthermore, brain magnetic resonance imaging, brainstem-evoked response audiometry, auditory brainstem response and chest X-ray were performed for Batten disease, Usher syndrome and situs inversus cases, respectively, based on availability of the facility. The families were enrolled following the standards of the Declaration of Helsinki for molecular genetic analysis. After the proband and all other affected and unaffected family members signed informed consent declarations, –5 ml of venous blood were drawn from each participating individual. Following our previously published protocol, genomic DNA extraction and quantification was performed at the Department of Zoology, Quaid-i-Azam University, Islamabad, Pakistan [27,28].

*Targeted exome sequencing and bioinformatic analysis:* DNA samples of two affected members from each enrolled family were used for capture panel sequencing at Baylor College of Medicine, Houston, TX. Exome-enriched genomic libraries were created following the manufacturer's instructions using the KAPA HyperPrep Kit (Roche, Basel, Switzerland). These libraries were then combined for targeted enrichment using the SureSelect Target Enrichment System for the Illumina Platform (Agilent, Santa Clara, CA) on a panel of 344 known and candidate inherited retinal disease-related genes (as detailed in our previous article [27]). Captured DNA was measured and sequenced using a Novaseq 6000 (Illumina, San Diego, CA). As mentioned in our earlier publications, variant calling, data alignment and filtering were performed at the Functional Genomics Core at Baylor College of Medicine [27,29]. Variant annotation and filtration was performed per recommendations of the American College of Medical Genetics and Genomics (ACMG). The HGMD, ClinVar and LOVD databases were searched and used to identify previously known pathogenic variants. Several in silico methods were used to assess novel variations for possible effects on protein function. Splice site variations, nonsense and frameshift variants were categorized as probable loss-of-function alleles. Sequence conservation and bioinformatic predictions were used to assess missense variants.

*Sanger sequencing and segregation test:* Online resource Primer3 was used to design primers for the Sanger sequencing validation of every potential pathogenic variation. Sanger sequencing and segregation testing was performed using the genomic DNA of proband and other affected/unaffected family members, depending on the availability of DNA samples.

## RESULTS

We recruited a cohort of 72 multi-generational consanguineous families, each with the segregating retinal phenotype, through Al-Shifa Trust Eye Hospital, Rawalpindi, Pakistan. Most of the enrolled families had multiple affected individuals. Upon molecular genetic analysis, 13 families were identified with disease-causing variants in syndromic IRD-related genes. Clinical data of the affected individuals of these syndromic families obtained at the time of enrollment are detailed in Table 1. Usher syndrome family data revealed that family RP057 had three, RP094 had two, RP182 had one, RP220 had seven and RP243 had six affected family members (Figure 1 and Appendix 1). The phenotypic onset in the proband of enrolled families ranged from birth to the second decade of life (Table 1). Among the families, the RP094 and RP182 probands (individuals III.I and IV.III) were affected by birth, individual IV.II in family RP057 had disease onset in the first decade of life, while individual V.XI in family RP220 and IV.IX in family RP243 were diagnosed in the second decade of life (Figure 1 and Appendix 1). In addition to the retinal phenotypes shared by the affected individuals of all families, such as night blindness, poor day vision and photosensitivity, affected individuals of Usher families also experienced progressive hearing loss. Astigmatism was observed in the affected individuals of family RP094, and strabismus and maculopathy were also observed in the RP243 family (Table 1). Fundus photographs of an affected individual of RP 243 (IV.IX) presenting waxy bone spicule with vascular attenuation are shown in Appendix 2. Brainstem-evoked response audiometry and auditory brainstem response testing of the proband (IV.II) of RP057 revealed bilateral severe-to-profound hearing impairment (Appendix 2).

In BBS families, each RP043, RP157 and RP164 family had three affected members, whereas RP173 had five affected cases. The proband (IV.V) of family RP043 and individual IV.II of RP173 were affected by birth (Table 1 and Appendix 3), while individuals III.XI of RP157 and V.III of RP164 were diagnosed in the first decade of life (Figure 2 and Appendix 3). BBS families showed the primary features of BBS such as retinal pigmentosa and polydactyly. A fundus image of the right and left eyes showing RP signs (Appendix 4) and photographs of the hand and foot showing postaxial polydactyly in affected individual IV.II of RP173 are shown in Appendix 4. Secondary features of BBS—macular dystrophy, low intellect and intellectual disability—were noted in family

RP164. Renal dysfunction was reported in affected members of family RP173.

Two affected members of family RD002 and three cases of RP155 had characteristics features of Batten disease/CLN including retinal degeneration, speech problems, seizures, loss of motor skills, cognitive decline, and behavioral and learning problems. The affected member V.II of RD002 had folded hands and weak bones (Figure 3). The brain magnetic resonance imaging scan of individual V.II of RD002 revealed generalized cerebral and cerebellar atrophic changes with associated volume loss not consistent with the age of patient, i.e., 17 years. The affected member IV.II of family RP155 has intellectual disability and remains mostly in an unconscious state (Figure 3). Medical records of all affected cases of RP067 revealed RP with situs inversus, and there are three affected males and one affected female (IV.XX) in RP067 (Figure 4). The chest X-rays of the affected individuals of RP067 revealed a reversed position of the heart and aorta. In families, the RP067 and RP155 probands (individuals IV.VII and IV.II) were affected by birth, and in family RD002, individual V.II had disease onset within the first decade of life. All affected members of family RP151 had onset of retinal phenotype by birth. They also had myopia, premature arthritis, aggressive behavior and slowly progressive hearing loss, and one affected member—IV.I—had a speaking defect (Table 1).

Capture panel sequencing led to the identification of 15 disease-causing variants, among which 9 were previously reported while the remaining 6 were novel (Table 2). Consistent with the mode of phenotypic inheritance, all Usher, BBS, CLNs and RP variants with situs inversus genes except c.12093C>A and c.9815C>T of *USH2A* were homozygous in affected cases. Variants c.12093C>A and c.9815C>T of *USH2A* segregated in a compound heterozygous form in family RP243 (Appendix 1). Furthermore, a heterozygous disease-causing variant c.247G>A of the *COL2A1* gene segregated in an autosomal dominant form with a disease phenotype in one family, i.e., RP151 (Appendix 5). All of the novel variants identified and previously reported, likely pathogenic/variant of uncertain significance/benign variants, were curated per ACMG guidelines and are listed in Table 2 and Table 3.

**Table 1. Demographic and clinical features of probands of 13 families described in this study.**

| Sr. No. | Family ID | Proband ID | Age in years at | | Ethnicity | Symptoms |
|---|---|---|---|---|---|---|
| | | | Enrollment | Onset | | |
| 1 | RP057 | IV.II | 12 | 7 | Punjabi | RP, Hearing loss, Speech defects, color vision problems, photophobia |
| 2 | RP094 | III.I | 25 | By birth | Punjabi | RP, Hearing loss, Speech defects, Astigmatism |
| 3 | RP182 | IV.III | 44 | By birth | Punjabi | RP, Hearing loss, Speech defects, color vision problems, photophobia |
| 4 | RP220 | V.V | 23 | 13 | Kashmiri | RP, Hearing loss, color vision problems, photophobia, Myopia |
| 5 | RP243 | IV.IX | 22 | 14 | Punjabi | RP, Hearing loss, color vision problems, photophobia, Strabismus, Maculopathy |
| 6 | RP043 | IV.V | 7 | By birth | Punjabi | RP, Polydactyly |
| 7 | RP157 | III.XIV | 23 | 6 | Pashtun | RP, Polydactyly, Astigmatism |
| 8 | RP164 | V.III | 8 | 8 | Pashtun | RP, Intellectual disability, Truncal obesity, Macular dystrophy |
| 9 | RP173 | IV.II | 16 | By birth | Pashtun | RP, Polydactyly, Intellectual disability, Rectal dysfunction |
| 10 | RD002 | V.II | 16 | 7 | Punjabi | RP, Seizures, Speech problems, Motor and cognitive decline, Behavioral and learning problems, Folded hands, Weak bones |
| 11 | RP155 | IV.II | 31 | By birth | Pashtun | RP, Seizures, Loss of motor skills, Speech problems, Cognitive decline, Mental Retardation |
| 12 | RP067 | IV.VII | 28 | By birth | Balochi | RP, Situs inversus, Photophobia, Sinusitis |
| 13 | RP151 | IV.V | 15 | By birth | Pashtun | RP, hearing loss, Myopia, Premature arthritis, Speaking defect, Aggressive behavior |

Abbreviations: ID: Identification, RP: Retinitis Pigmentosa, CLNs: Ceroid Lipofuscinoses Neuronal, NI: Not Investigated.

Disease-causing variants in Usher syndrome genes were found in the *USH2A*, *MYO7A* and *PCDH15* genes in five families (Table 2, Figure 1 and Appendix 1). *USH2A* gene variants were associated with disease phenotype in two unrelated families (RP220 and RP243; Figure 1 and Appendix 1). A novel homozygous substitution, c.1143G>C, was found to be segregating disease phenotype in five affected and four unaffected individuals of the RP220 family (Figure 1C). This variant substitutes glutamine to histidine at position 381 in the protein, i.e., p.(Gln381His; Figures 1C and Figure 3C). This variant is absent from gnomAD, ClinVar and dbSNP but present in LOVD. Two heterozygous pathogenic variants in the *USH2A* gene segregated in RP243, with one a truncating transversion, i.e., c.12093C>A causing p.(Tyr4031Ter), which is listed as pathogenic in ClinVar and dbSNP (rs55921307); and the other is a known missense pathogenic variant c.9815C>T:p.(Pro3272Leu) listed in ClinVar and dbSNP (rs104893791). Segregation testing for the five affected and two unaffected family members confirmed the perfect segregation of both *USH2A* variants in a compound heterozygous manner with the disease phenotype (Appendix 1). Interestingly, a nonsyndromic RP-affected female (III.I) of family

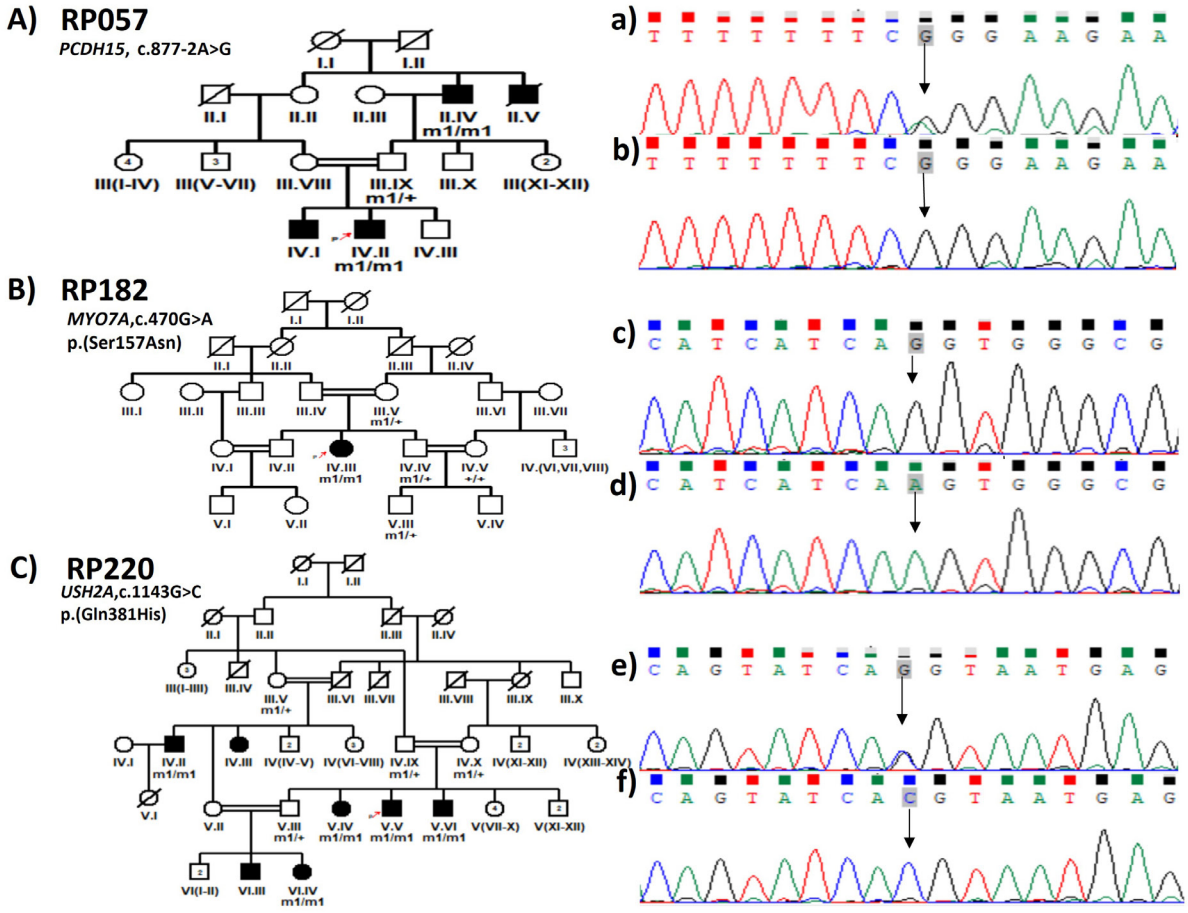


Figure 1. Three pedigrees in which novel homozygous pathogenic variants were identified in Usher syndrome-associated genes in this study along with representative sequence chromatograms. Empty squares and circles indicate unaffected males and females, respectively. Filled shapes indicate affected individuals. The symbol labeled with a red arrow in each pedigree highlights the proband. Double lines indicate a consanguineous union. **A**: Pedigree of the RP057 family showing segregation of the novel *PCDH15* splice site variant, i.e., c.877–2A>G in an autosomal recessive manner; (a) shows the sequence chromatogram highlighting carrier status A/G and (b) shows a homozygous mutant allele G. **B**: Pedigree of the RP182 family showing segregation of the novel *MYO7A* single-nucleotide substitution, i.e., c. 470G>A, in an autosomal recessive manner; (c) shows the sequence chromatogram highlighting wild-type allele G and (d) shows a homozygous mutant allele A. **C**: Pedigree of the RP220 family showing the segregation of the novel *USH2A* single-nucleotide substitution, i.e., c. 1143G>C, in an autosomal recessive manner; (e) shows the sequence chromatogram highlighting carrier status G/C and (f) shows homozygous mutant allele C.

RP243 did not carry *USH2A* variants found in the other five affected cases; instead she was homozygous for a previously reported missense variant, i.e., c.448G>A; p. (Glu150Lys) of the *RHO* gene (Appendix 1). This variant is reported in the gnomAD (v.2.1.1) database only within the South Asian population with an estimated frequency of 0.00004772 and is listed in ClinVar (variation ID: 13,046) as pathogenic by multiple submitters for the autosomal recessive RP phenotype.

Two homozygous missense disease-causing variants in the *MYO7A* gene, i.e., c.3508G>A: p.(Glu1170Lys) and c.470G>A: p.(Ser157Asn), were found in families RP094 and RP182, respectively (Figure 1 and Appendix 1). Consistent with the molecular diagnosis, patients from both families exhibited RP and hearing loss. The p.(Glu1170Lys) variant identified in RP094 is reported in ClinVar as a pathogenic variant with a minor allele frequency of 0.00002012 in gnomAD (v.2.1.1). Segregation testing was performed on the two affected and two unaffected family members, and perfect segregation between mutation and disease phenotype was observed (Appendix 1). Similarly, one affected case of RP182 was homozygous for the c.470G>A variant while controls were either homozygous for the wild-type allele or heterozygous carriers of the disease allele (Figure 1B). The c.470G>A: p.(Ser157Asn) variant identified in RP182 is a novel report, as this is absent from gnomAD (v.2.1.1) and other databases including ClinVar, dbSNP and LOVD.

The *PCDH15* gene, another Usher syndrome gene, was mutated in family RP057. All patients of family RP057 had speaking and hearing defects (Table 1). Capture panel sequencing data analysis revealed a novel homozygous missense variant, c.877–2A>G, in chromosome 10—55996693T>C in intron 8 of the *PCDH15* gene, which is predicted to cause splice site defects (Table 2). Similarly, segregation testing in two affected and one unaffected family member indicated the segregation of identified variants with the Usher syndrome phenotype in RP057 (Figure 1A). This variant is absent from gnomAD (v.2.1.1) and all other databases, including ClinVar, and is likely to affect splicing, with SpliceAI scores for donor loss (delta score of 0.50, −110 bp), acceptor gain (delta score of 0.26, −6 bp) and acceptor loss (delta score of 0.1, −2 bp).

Among the BBS genes, three disease-causing variants in the *ARL6* gene were found to be segregated in families RP043, RP164 and RP173, respectively (Table 2, Figure 2 and Appendix 3). A previously reported pathogenic missense homozygous variant, i.e., c.281C>T: p.(ILe94Thr) with a minor allele frequency of 0.00003186 in gnomAD (v.2.1.1) was shown to be segregated in RP043 (Appendix 3). This variant is reported in ClinVar (variation ID: 438,186) as

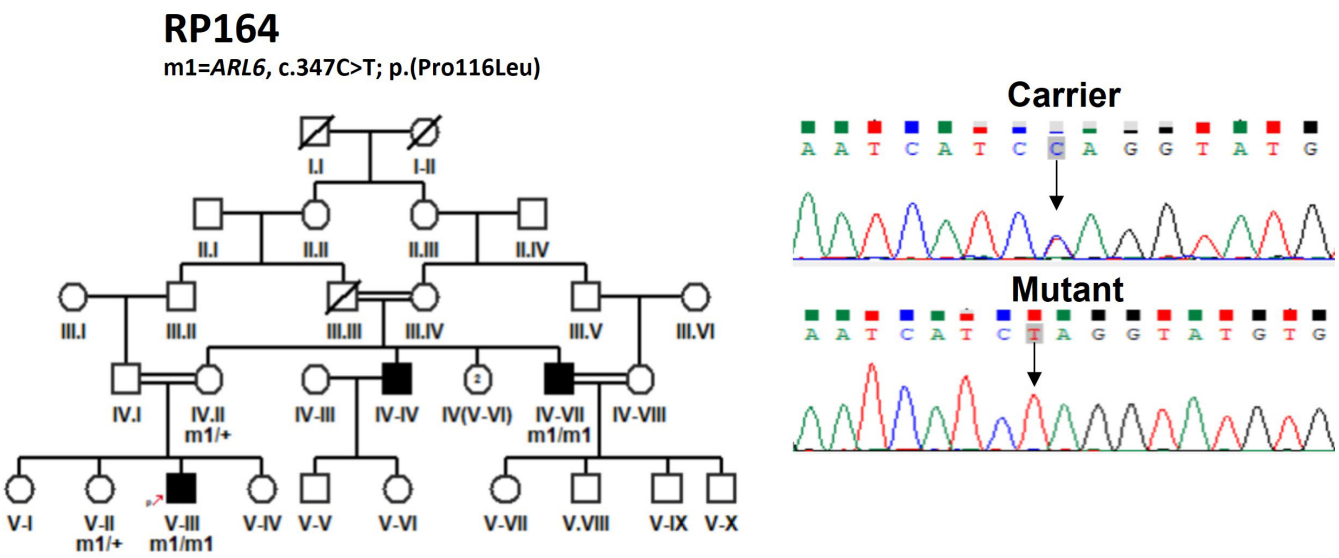


Figure 2. Pedigree of the RP164 family along with sequence chromatograms. Left. Pedigree of the RP164 family in which a novel homozygous pathogenic variant, i.e., c.347C>T, leads to a missense substitution, i.e., p. Pro116Leu, being identified in the BBS3 (*ARL6*) gene along with representative sequence chromatograms. Empty squares and circles indicate unaffected males and females, respectively. Filled shapes indicate affected individuals. The symbol labeled with a red arrow highlights the proband. Double lines indicate a consanguineous union. Right. Pedigree of RP164 family showing the segregation of a novel variant, i.e., c.347C>T, in an autosomal recessive manner. The sequence chromatogram highlighting carrier status as well as a homozygous mutant allele is shown on the left.

pathogenic for the BBS3 phenotype and likely pathogenic for the RP phenotype. A novel homozygous substitution in exon 5 of the *ARL6* gene, i.e., c.347C>T: p.(Gln352Pro) was found in family RP164 (Figure 2). This variant is absent from the gnomAD (v.2.1.1), ClinVar, LOVD and dbSNP databases. Segregation of this variant with disease was observed by genotyping two affected and two unaffected family members, where affected members were homozygous for the variant, while unaffected members were carriers of the mutant allele (Figure 2). In RP173, a homozygous substitution, i.e., c.534A>G: p.(Gln178=) in exon 7 of the *ARL6* gene segregated with the phenotype (Appendix 3). This variant is reported in gnomAD (v.2.1.1) with a minor allele frequency of 0.000007960 and as pathogenic in ClinVar (variation ID: 1,805,423) for the BBS3 phenotype and is predicted to affect the splicing of pre-mRNA transcripts, as suggested by SpliceAI scores for acceptor loss (delta score of 0.71, −54 bp) and donor loss (delta score of 0.87, −1 bp). Sanger sequencing confirmed five affected family members as homozygous and four unaffected family members as heterozygous carriers of mutant allele, further supporting the pathogenicity of this variant. The affected individuals of all three families with *ARL6* variants had severe phenotypes, as all affected family members recorded RP and polydactyly at birth. The proband of RP173 was 16 years old at the time of enrollment for this study and had rectal dysfunction with low intellect (Table 1).

In family RP157, homozygous missense deleterious variant c.1055A>C: p.(Gln352Pro) was detected in exon 2 of the BBS*12* gene (Appendix 3). This variant is reported in gnomAD (v.2.1.1) with a minor allele frequency of 0.00004775 and in ClinVar (variation ID: 560,429) with conflicting interpretations of pathogenicity, i.e., pathogenic, likely pathogenic and variant of uncertain significance by multiple submitters for the BBS12 phenotype. In this study, we detected perfect segregation of this variant with phenotype in two affected and one control member of family RP157, adding to the evidence of pathogenicity per ACMG guidelines. Affected members

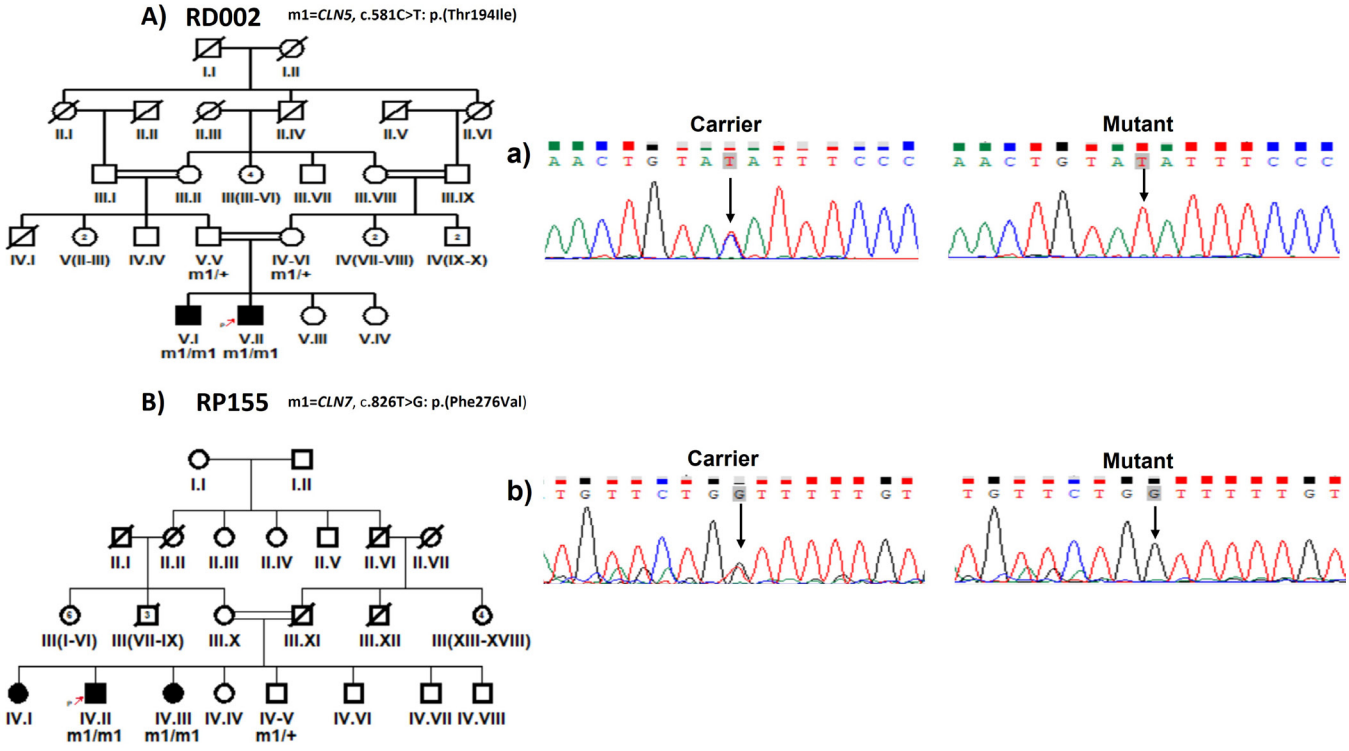


Figure 3. Two pedigrees in which homozygous pathogenic variants were identified in Batten disease-associated genes in this study along with representative sequence chromatograms. Empty squares and circles indicate unaffected males and females, respectively. Filled shapes indicate affected individuals. The symbol labeled with a red arrow in each pedigree highlights the proband. Double lines indicate a consanguineous union. **A**: Pedigree of the RD002 family showing segregation of the novel *CLN5* missense variant, i.e., c.581C>T, in an autosomal recessive manner; (a) shows a sequence chromatogram highlighting carrier status and a homozygous mutant allele on the right and left side, respectively. **B**: Pedigree of the RP155 family showing segregation of the *MFSD8/CLN7* single-nucleotide substitution, i.e., c. 826T>G, in an autosomal recessive manner; (b) shows a sequence chromatogram highlighting carrier status and a homozygous mutant allele on the right and left side, respectively.

of RP157 had astigmatism and polydactyly with initial complaints of retinal detachment and blurred vision (Table 1).

Two families, RD002 and RP155, showed segregating missense variants in Batten disease genes, i.e., *CLN5* and *MFSD8/CLN7*, respectively (Table 2 and Figure 3). In RD002, a homozygous single-base transition, i.e., c.581C>T leading to p.(Thr194Ile), missense change was found segregating in two affected and two phenotypically unaffected members. This variant is absent from gnomAD (v.2.1.1) and other databases including ClinVar. Similarly, in RP155, a single-base substitution, i.e., c.826T>G causing p.(Phe276Val) in *MFSD8/CLN7*, was segregated as an autosomal recessive variant with the Batten disease phenotype. This variant is reported in gnomAD (v.2.1.1) as a single allele of South Asian ancestry with a minor allele frequency of 0.000003978 and in ClinVar (variation ID: 3,294,568) as a variant of uncertain significance by a single submitter for inborn genetic disease. In family RP067, a novel splice site variant of the *ARL2BP* gene was found to be segregated with the RP and situs inversus phenotype in a recessive manner (Figure 4). This variant is likely to affect splicing, with Splice AI scores of 0.96 for acceptors loss and 0.99 for donor loss. This variant is absent from gnomAD (v.2.1.1) and other databases including ClinVar.

Finally, in family RP151, a disease-causing single-nucleotide transition, c.247G>A, leading to glycine to arginine substitution, i.e., p.(Gly83Arg) in the *COL2A1* gene, was segregated in an autosomal dominant manner with an ocular phenotype (Table 2 and Appendix 4). This variant is found in gnomAD (v.2.1.1) with a minor allele frequency of 0.00002003 and is listed in ClinVar (variation ID: 964324) as likely to be benign by a single submitter of unknown disease status. However, segregation testing in the present study confirmed perfect segregation of this hemizygous variant with the SS phenotype in three affected males, whereas a phenotypically normal female was homozygous for the wild-type allele, as shown in (Appendix 3; Appendix 5), thereby providing evidence of pathogenicity (Table 3).

In conclusion, the six disease-causing variants (*USH2A*: c.1143G>C, p.(Gln381His); *MYO7A*: c.470G>A, p.(Ser157Asn); *PCDH15*: c.877–2A>G, *ARL6*: c.347C>T, p.(Pro116Leu), *CLN5*: c.581C>T, p.(Thr194Ile) and *ARL2BP*: c.100+1G>T) identified in our study cohort are novel findings. Segregation results as well as chromatograms of all variants are given along the family tree of each family in Figure 1, Figure 2, Figure 3 and Figure 4 and Appendix 1, Appendix 2 and Appendix 3. Clustal W analysis of four novel amino acid substitutions identified in *ARL6*, i.e., p.(Pro116Leu), *MYO7A*, i.e., p.(Ser157Asn), *USH2A*, i.e., p.(Gln381His) and *CLN5*, i.e., p.(Thr194Ile) revealed evolutionary conservation across species (Figure 5A-D).

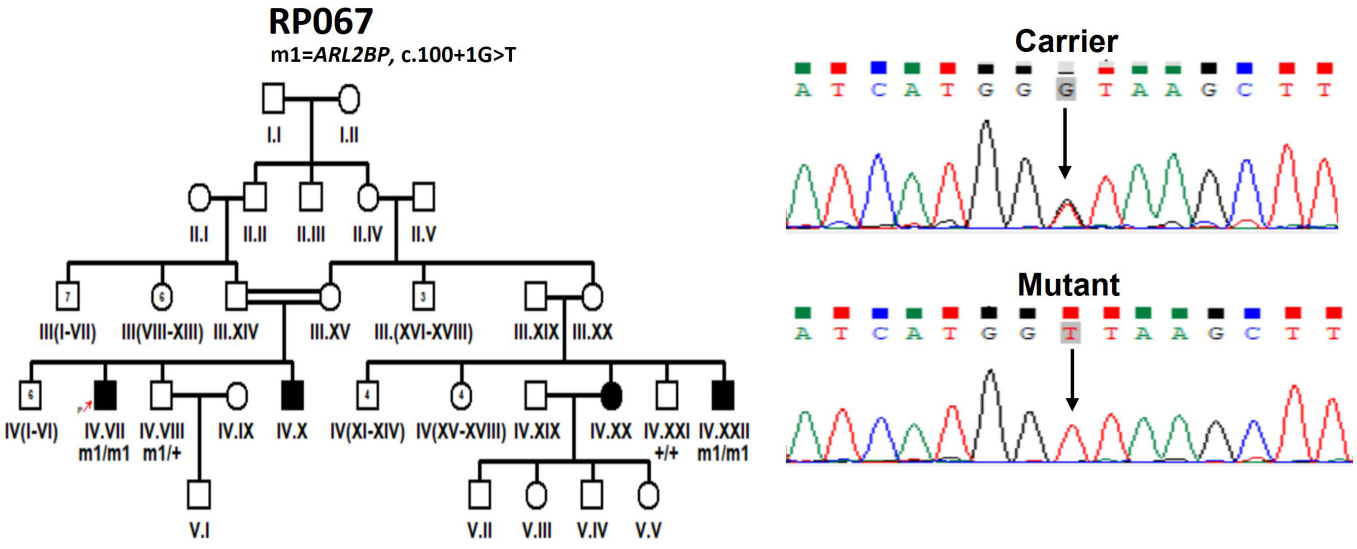


Figure 4. Pedigree of the RP067 family along with sequence chromatograms. Left: Pedigree of the RP067 family in which a novel homozygous pathogenic variant, i.e., c.100+1G>T, was identified in the *ARL2BP* gene segregating with RP and situs inversus, along with representative sequence chromatograms. Empty squares and circles indicate unaffected males and females, respectively. Filled shapes indicate affected individuals. The symbol labeled with a red arrow highlights the proband. Double lines indicate a consanguineous union. Right: Pedigree of the RP067 family showing segregation of a novel variant, i.e., c.100+1G>T, in an autosomal recessive manner. The sequence chromatogram highlights carrier status and a homozygous mutant allele is shown on the left.

Table 2. List of identified variants in syndromic RP genes in a Pakistani cohort of 10 families.

| Sr. No. | Family ID | Accession Number | Gene | Zygosity | Variant | Nucleotide change | Coding impact | db SNP ID | ClinVar ID/classification |
|---|---|---|---|---|---|---|---|---|---|
| **1** | **RP057** | **NM_001384140.1** | *PCDH 15* | **Homo** | **CHR10:55996693T>C** | **c.877–2A>G** | **Splice site** | **NA** | **NA** |
| 2 | RP094 | NM_000260.4 | *MYO7A* | Homo | CHR11:76900393G>A | c.3508G>A | p.(Glu1170Lys) | rs111033214 | 43,208/P |
| 3 | RP182 | NM_000260.4 | *MYO7A* | Homo | CHR11:76867137G>A | c.470G>A | p.(Ser157Asn) | NA | NA |
| 4 | RP 220 | NM_206933.4 | *USH2A* | Homo | CHR1:216498647C>G | c.1143G>C | p.(Gln381His) | NA | NA |
| | | NM_000539.3 | *RHO* | Homo | CHR3:129249805G>A | c.448G>A | p(Glu150Lys) | rs104893791 | 13,046/P |
| 5 | RP243 | NM_206933.4 | *USH2A* | Hetero | CHR1:215853692G>T | c.12093C>A | p.(Tyr4031Ter) | rs55921307 | 5,446,112/P |
| | | NM_206933.4 | *USH2A* | Hetero | CHR1:215972392G>A | c.9815C>T | p.(Pro3272Leu) | rs764182950 | 553,424/P |
| 6 | RP043 | NM_001278293.3 | *ARL6* | Homo | CHR3:97503825T>C | c.281C>T | p.(Ile94Thr) | rs771054395 | 438,186/P |
| 7 | RP157 | NM_152618.3 | *BBS12* | Homo | CHR4:123664102A>C | c.1055A>C | p.(Gln352Pro) | rs767068756 | 560,429/LP |
| 8 | RP164 | NM_001278293.3 | *ARL6* | Homo | CHR3:97503891C>T | c.347C>T | p.(Pro116Leu) | NA | NA |
| 9 | RP173 | NM_001278293.3 | *ARL6* | Homo | CHR3:97510669A>G | c.534A>G | p.(Gln178=) | rs756341249 | 1,805,423/P |
| 10 | RD002 | NM_006493.2 | CLN5 | Homo | chr13:77570131 C>T | c.581C>T | p.(Thr194Ile) | rs113944597 | NA |
| 11 | RP155 | NM_001371596.2 | MFSD8/CLN7 | Homo | chr4:128854177 A>C | c.826T>G | p.(Phe276Val) | rs756815122 | 3,294,568/VUS |
| 12 | RP067 | NM_012106.4 | ARL2BP | Homo | chr16:57280054 G>T | c.100+1G>T | Splice site | NA | NA |
| 13 | RP151 | NM_001844 | *COL2A1* | Homo | CHR12.48393747C>T | c.247G>A | p.(Gly83Arg) | rs762911032 | 964,324/LB |

Sequence variant Nomenclature was obtained according to the guidelines of the Human Genome Variation Society (HGVS) by using Mutalyzer (https://mutalyzer.nl/). The position of variants is according to GRCh37/hg19 reference genome assembly.

Table 3. Curated classification of novel and previously reported likely pathogenic/ variant of uncertain significance/benign variants as per ACMG guidelines.

| Sr. No. | Gene | | Variant | Variant interpretation | | |
|---|---|---|---|---|---|---|
| | ID | Accession number | | Clin Var ID/classification | Codes met | Curated classification |
| 1 | *PCDH 15* | NM_001384140.1 | CHR10:55996693T>C | NA | PM2, PVS1, PP4, PP1, PP3 | Pathogenic |
| 2 | *MYO7A* | NM_000260.4 | CHR11:76867137G>A | NA | PM2, PP2, PP4, PP3 | Pathogenic |
| 3 | *USH2A* | NM_206933.4 | CHR1:216498647C>G | NA | PM2, PP1, PP2, PP4 | Likely pathogenic |
| 4 | *BBS12* | NM_152618.3 | CHR4:123664102A>C | 560,429/Likely Pathogenic | PM2, PP1, PP4 | Likely Pathogenic |
| 5 | *ARL6* | NM_001278293.3 | CHR3:97503891C>T | NA | PM2, PP1, PP4 | Likely pathogenic |
| 6 | *CLN5* | NM_006493.2 | CHR13:77570131 C>T | NA | PM2, PP1, PP2, PP3, PP4 | Likely pathogenic |
| 7 | *MFSD8/CLN7* | NM_001371596.2 | CHR4:128854177 A>C | 3,294,568/Uncertain significance | PM2, PP1, PP2, PP3, PP4 | Likely pathogenic |
| 8 | *ARL2BP* | NM_012106.4 | CHR16:57280054 G>T | NA | PM2, PVS1, PP3, PP4, PP1 | Pathogenic |
| 9 | *COL2A1* | NM_001844 | CHR12.48393747C>T | 964,324/Likely Benign | BS1, PP3, PP1, PP4 | Likely pathogenic |

PM2: Pathogenic moderate 2 [Absent from controls (or at extremely low frequency if recessive) in Exome Sequencing Project, 1000 Genomes Project, or Exome Aggregation Consortium] PVS1: Pathogenic very strong [null variant (nonsense, frameshift, canonical ±1 or 2 splice sites, initiation codon, single or multiexon deletion) in a gene here LOF is a known mechanism of disease)] PP1:[ Cosegregation with disease in multiple affected family members in a gene definitively known to cause disease] PP2: Pathogenic supporting 2 [Missense variant in a gene that has a low rate of benign missense variation and in which missense variants are a common mechanism of disease] PP3: Pathogenic supporting 3 [Multiple lines of computational evidence support a deleterious effect on the gene or gene product (conservation, evolutionary, splicing impact, etc.)] PP4: Pathogenic supporting 4 [Patient's phenotype or family history is highly specific for a disease with a single genetic etiology] BS1: Benign Supporting 1 [Allele frequency is greater than expected for disorder].

## DISCUSSION

Developing therapeutic measures for inherited eye diseases requires a detailed understanding of the disease pathways through the identification of genetic mutations [27,30–32]. Current therapeutic strategies include delivering a wild-type (nonmutated) copy of the affected gene [33] or precisely modified nucleotide sequences within the genome through genome editing technologies [34]. However, due to genetic heterogeneity, i.e., the involvement of multiple genes in a disease phenotype, mutations within the same gene causing different phenotypes and mutations in different genes causing similar clinical phenotypes, it is important to understand the precise genetic defects to develop suitable treatment strategies for these blinding conditions [35,36]. All three modes of inheritance—dominant, recessive and X-linked—have been reported for IRDs [27,32]. However, recessive forms are more common in populations where endogamy is a social preference [32,37], including Pakistan [27,32,38,39]. Studies have revealed several genetic mutations causing IRDs from Pakistan, but these data are too limited compared with the high prevalence of these disorders in our population [27,32,38]. Thus, here we used a cost-effective panel sequencing approach followed by Sanger sequencing for segregation testing to reveal the mutation spectrum of 72 IRD-affected Pakistani families. Our results identified disease-causing variants of syndromic IRD genes in 13 analyzed families (13/72; 18%) with significant genetic and phenotypic heterogeneity.

Interesting observations from this study include the presence of compound heterozygous disease-causing variants of *USH2A* and a homozygous missense pathogenic variant of

*RHO* in five affected cases and one affected case, respectively, in the same family RP243 (Appendix 1). Pathogenic variant c.448G>A: p.(Glu150Lys) of the *RHO* gene was present in one nonsyndromic RP patient (individual III.I; Appendix 1) and it was also previously reported in three consanguineous Pakistani families and an Indian family with segregated autosomal recessive RP [40–42]. A heterozygous pathogenic variant of the *USH2A* gene, i.e., c.12093C>A, was previously reported in compound heterozygous form along with a heterozygous splice site variant, i.e., 12,295–3T>A in a male European Usher patient [43]. Similarly, the other *USH2A* heterozygous variant, c.9815C>T, identified in RP243, was also previously detected as a heterozygous allele in an Italian autosomal recessive RP patient, a Dutch Usher II patient and a Chinese Usher II patient [44–46]. Furthermore, the c.1143G>C transversion leading to a glutamine-to-histidine substitution at the 381 position of the Usherin protein identified as a homozygous variant in affected cases of family RP220 in this study was previously present as a heterozygous allele segregating in a compound heterozygous manner with another heterozygous splice site substitution, i.e., c.8559-2A>G, in a sporadic Chinese Usher patient of Han ethnicity [47]. However, in family RP220, segregation of this variant in autosomal recessive form with disease phenotype was confirmed by genotyping five affected and four unaffected individuals, elevating evidence of the pathogenicity of this variant per ACMG criteria (Figure 1C and Table 3).

USH1 is the most severe form of Usher syndrome and is reported to account for approximately 25%–44% of all cases of Usher syndrome globally [48]; however, in this study disease-causing variants in Usher type 1 (USH1)–related genes, i.e., *PCDH15* and *MYO7A*, were found in three out of five (60%) Usher-segregating families, highlighting the unique mutation spectrum of this disorder in the Pakistani population. Furthermore, in the current study we identified pathogenic variants of the *BBS3* (*ARL6*) gene in three out of four (75%) BBS families, which contrasts with previous reports indicating *BBS6* as a frequently mutated BBS gene in families from Pakistan [39,49]. However, this variability may be due to the different ethnic lineages of families enrolled in previous studies as well as this study.

Identification of a novel pathogenic variant of the *ARL6* gene, i.e., c.347C>T causing p.(Pro116Leu), inherited recessively in three patients of family RP164 reaffirms the genetic heterogeneity of *BBS3* in the Pakistani population. Initial clinical assessment of the proband of RP164 indicated nonsyndromic RP; however, examination of all other affected individuals showed intellectual disability in one patient (V.III; Figure 2). The phenotypic variability across different affected cases may be due to the pleiotropic nature of BBS, as a wide range of clinical variability has been observed both within and between families [6]. Previously, nonsyndromic RP was reported in Saudi Arabian patients carrying a homozygous missense variant (p.Ala89Val) in the *ARL6* gene [50]. The occurrence of different clinical phenotypes due to the same mutation suggests a role of the complex genetic background of each patient in these heterogeneous clinical outcomes. Furthermore, our molecular genetic testing assisted with the diagnosis of RP164 (Table 1 and Figure 2) and suggested monitoring of all affected cases of this family for the risk of cardiac and kidney issues for the timely management of patients.

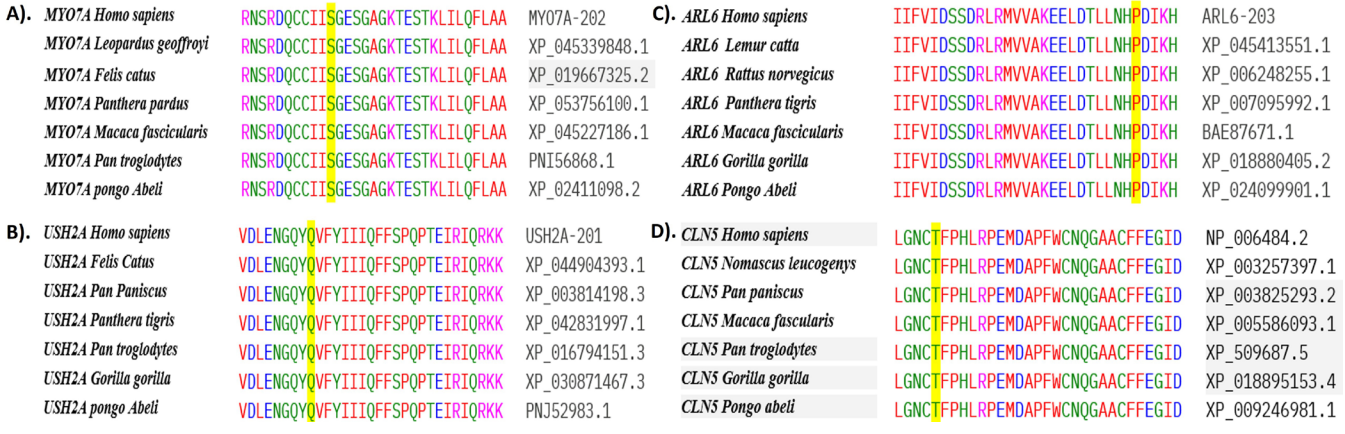


Figure 5. Clustal Omega multiple-sequence alignment showing the evolutionary conservation of amino acids across species for which novel substitutions (highlighted red) were identified in this study. **A**: Conservation of serine at position 157 in the *MYO7A* protein. **B**: Conservation of glutamine at position 381 in the *USH2A* protein. **C**: Conservation of proline at position 116 in the *ARL6* protein. **D**: Conservation of threonine at position 194 in the *CLN5* protein.

In this study, we identified disease-causing variants in CLN (Batten disease) proteins that localized to lysosomes, i.e., *CLN5* and *MFSD8/CLN7*, segregating with progressive retinal degeneration along with cognitive and motor regression, as well as epileptic abnormalities in family RD002 and RP155, respectively (Table 2 and Figure 3) [51]. To date, a total of three disease-causing mutations (c.1072_1073delTT [p.Leu358AlafsX4], c.925_926del [p.Leu309AlafsTer4] and c.477T>C [p.Cys159Arg]) in exon 4 of the *CLN5* gene have been reported in Batten disease cases of Pakistani decent [52,53]. Identification of a likely novel pathogenic variant in exon 4 of the *CLN5* gene causing a missense change, i.e., p.Thr194Ile in family RD002 in the present study, highlights exon 4 as a hot-spot exon for the molecular genetic analysis of Batten disease cases of Pakistani origin. However, the missense variant, i.e., p.(Phe276Val) of MFSD8/CLN7 segregating in family RP155 has been reported in ClinVar (variation ID: 3,294,568) for inborn genetic disease with no further details of clinical significance/inheritance; however, our study provides the first evidence of the inheritance of this variant with the Batten disease phenotype in a Pashtun sibship in Pakistan (Figure 3).

In this study, the main limitation/s explaining genetic variants to phenotypic diversity is the unavailability of detailed clinical reports including electroretinography, audiometry of all Usher syndrome cases, and other necessary clinical tests to confirm BBS and SS phenotypes. In family RP151, all affected cases had vision and hearing impairments, as well as premature joint pain, which are symptoms of SS (Table 1 and Appendix 5), a connective tissue disorder [25]. However, the family was not willing to participate in detailed clinical examination to rule out the type of hearing loss; i.e., conductive or sensorineural assessment, as well as testing for degenerative joint disease. However, in this context, genetic screening in this study assisted with diagnosis. Our study highlights the need to invest in better diagnostic equipment, laboratory capabilities and electronic health record systems in underserved communities to capture more comprehensive clinical data for future research for a complete understanding of disease mechanisms and potential therapeutic targets. To the best of our knowledge, this is the first report of genetic screening for *MFSD8/CLN7*, *ARL2BP* and *COL2A1* in Pakistani families inheriting Batten disease (RP155), RP along with situs inversus (RP067) and Stickler syndrome (RP151), respectively. Our data support genetic testing of patients with inherited disorders in Pakistan for accurate diagnosis and early interventions to improve the quality of life of affected families.

## APPENDIX 1. SUPPLEMENTARY FIGURE 1.

To access the data, click or select the words "Appendix 1." Two pedigrees in which previously known pathogenic variants were identified in Usher syndrome associated genes in this study along with representative sequence chromatograms. Empty squares and circles show the unaffected males and females, respectively. The filled shapes show the affected individuals. The symbol labeled with a red arrow in each pedigree highlights the proband. Double lines indicate the consanguineous union. A) Pedigree of RP094 family showing the segregation of the *MYO7A* single nucleotide substitution i.e., c.3508G>A in an autosomal recessive manner however (a) shows the sequence chromatogram highlighting carrier status and a homozygous mutant allele on the right and left side respectively. B) Pedigree of RP243 family showing the segregation of the two heterozygous *USH2A* single nucleotide substitutions i.e., c. 12093C>A and c.9815C>T in a compound heterozygous manner in five affected cases as well as presence of a homozygous pathogenic RHO substitution c.448G>A in one non-syndromic RP affected individual (III.I) however (b-c) shows the sequence chromatograms highlighting wild-type and heterozygous mutant allele c. 12093C>A and c.9815C>T of *USH2A* on the right and left side respectively. d) shows the sequence chromatogram highlighting wild-type status and a homozygous mutant allele of RHO i.e., c.448G>A on the right and left side respectively.

## APPENDIX 2. SUPPLEMENTARY FIGURE 2.

To access the data, click or select the words "Appendix 2." (A) Fundus photographs of right and left eye of an affected individual (IV. IX) of RP243 showing pale optic disc, bony spicules and thin blood vessels characteristic of RP phenotype and (B) ABR testing results of right and left ear of an affected individual (IV. II) of RP057. The x-axis depicts hearing level in dB (decibels).

## APPENDIX 3. SUPPLEMENTARY FIGURE 3.

To access the data, click or select the words "Appendix 3." Three pedigrees in which previously known pathogenic variants were identified in BBS syndrome associated genes in this study along with representative sequence chromatograms. Empty squares and circles show the unaffected males and females, respectively. The filled shapes show the affected individuals. The symbol labeled with a red arrow in each pedigree highlights the proband. Double lines indicate the consanguineous union. A) Pedigree of RP043 family showing the segregation of the *ARL6* single nucleotide substitution i.e., c.281C>T in an autosomal recessive manner however (a) shows the sequence chromatogram highlighting wild-type

and a homozygous mutant allele on the right and left side respectively. B) Pedigree of RP157 family showing the segregation of the *BBS12* single nucleotide substitution i.e., c.1055A>C in an autosomal recessive manner however (b) shows the sequence chromatogram highlighting carrier and a homozygous mutant allele on the right and left side respectively. C) Pedigree of RP173 family showing the segregation of the *ARL6* single nucleotide substitution i.e., c.534A>G in an autosomal recessive manner however (b) shows the sequence chromatogram highlighting carrier and a homozygous mutant allele on the right and left side respectively.

## APPENDIX 4. SUPPLEMENTARY FIGURE 5.

To access the data, click or select the words "Appendix 4." (A) Fundus photographs of right and left eye of an affected individual (IV. II) of RP173 showing pale optic disc, bony spicules and thin blood vessels characteristic of RP phenotype and (B) Photograph of right foot showing postaxial/fibular polydactyly phenotype and of right hand showing postaxial/ulnar polydactyly phenotype in an affected individual (IV. II) of RP173 characteristic of Bardet-Biedl Syndrome.

## APPENDIX 5. SUPPLEMENTARY FIGURE 4

To access the data, click or select the words "Appendix 5." Pedigree drawings of RP151 (right side) along with sequence chromatograms showing wild-type and heterozygous mutant allele (left side) i.e., c. 247G>A of *COL2A1* gene. The variant is segregating in an autosomal dominant pattern with Stickler syndrome phenotype. Squares and circles denote males and females respectively. Filled symbols show affected while unfilled symbols show unaffected individuals. The symbol labeled with a red arrow in pedigree highlights the proband. Double lines indicate the consanguineous union.

## ACKNOWLEDGMENTS

We thank patients and their families for their participation in this study. Author contribution: Sabika Firasat, Kiran Afshan, and Rui Chen contributed to the conceptualization and design. Sumaira Altaf performed clinical evaluations of patients. Aleesha Asghar, Sumbal Wazir, Shehzeen Fatima, Hussan Bilal, Muhammad Shoaib and Saqib Ur Rehman enrolled families and collected data. Aleesha Asghar, Sumbal Wazir, Shehzeen Fatima, Hussan Bilal, Muhammad Shoaib, Saqib Ur Rehman, Yumei Li, and Sabika Firasat performed experiments and data analysis. Aleesha Asghar, Yumei Li, Kiran Afshan, Sabika Firasat, and Rui Chen prepared the first draft of the manuscript. All authors read and approved the content and submission of the final manuscript. Conflict of interest: We have no conflict of interest. Funding: This study was financially supported (in part) by the University Research Fund (URF) from Quaid-i-Azam University, Islamabad, Pakistan to Sabika Firasat. This work is also supported by grants from the National Eye Institute [R01EY022356, R01EY018571, R01EY002520, P30EY010572, R01EY09076, R01EY030499]; Retinal Research Foundation; NIH shared instrument grant [S10OD023469] to Rui Chen. The authors acknowledge support to the Gavin Herbert Eye Institute at the University of California, Irvine from an unrestricted grant from Research to Prevent Blindness and from NIH grant P30 R01EY034070 to Rui Chen. Dr. Chen (ruic20@uci.edu) and Dr. Firasat (sabika.firasat@qau.edu.pk) are co-corresponding authors for this paper.

## REFERENCES

1. Lee BJH, Tham Y-C, Tan T-E, Bylstra Y, Lim WK, Jain K, Chan CM, Mathur R, Cheung CMG, Fenner BJ. Characterizing the genotypic spectrum of retinitis pigmentosa in East Asian populations: a systematic review. Ophthalmic Genet 2023; 44:109-18. [PMID: 36856324].
2. Ehrenberg M, Weiss S, Orenstein N, Goldenberg-Cohen N, Ben-Yosef T. The co-occurrence of rare non-ocular phenotypes in patients with inherited retinal degenerations. Mol Vis 2019; 25:691-702. [PMID: 31814694].
3. Tatour Y, Ben-Yosef T. Syndromic inherited retinal diseases: genetic, clinical and diagnostic aspects. Diagnostics (Basel) 2020; 10:779-[PMID: 33023209].
4. Janakiraman N, Badrinarayanan L, Ratra D, Elchuri SV. One Health Approach for Eye Care: Is It a Boon or Hype? One Health: Human, Animal, and Environment Triad. 2023:221–41.
5. Holanda IP, Rim PHH, Guaragna MS, Gil-da-Silva-Lopes VL, Steiner CE, Steiner CE. Rare Genomes Project Consortium. Syndromic Retinitis Pigmentosa: A 15-Patient Study. Genes (Basel) 2024; 15:516-[PMID: 38674450].
6. Beales PL, Elcioglu N, Woolf AS, Parker D, Flinter FA. New criteria for improved diagnosis of Bardet-Biedl syndrome: results of a population survey. J Med Genet 1999; 36:437-46. [PMID: 10874630].
7. Mitchison HM, Valente EM. Motile and non-motile cilia in human pathology: from function to phenotypes. J Pathol 2017; 241:294-309. [PMID: 27859258].
8. Forsyth R, Gunay-Aygun M. Bardet-Biedl Syndrome Overview. 2003 Jul 14 [updated 2023 Mar 23]. In: Adam MP, Feldman J, Mirzaa GM, Pagon RA, Wallace SE, Amemiya A, editors. GeneReviews® [Internet]. Seattle (WA): University of Washington, Seattle; 1993–2025.
9. Zacchia M, Blanco FDV, Torella A, Raucci R, Blasio G, Onore ME, Marchese E, Trepiccione F, Vitagliano C, Iorio VD, Alessandra P, Simonelli F, Nigro V, Capasso G, Viggiano D. Urine concentrating defect as presenting sign of progressive

renal failure in Bardet-Biedl syndrome patients. Clin Kidney J 2020; 14:1545-51. [PMID: 34084454].

10. Manara E, Paolacci S, D'Esposito F, Abeshi A, Ziccardi L, Falsini B, Colombo L, Iarossi G, Pilotta A, Boccone L, Guerri G, Monica M, Marta B, Maltese PE, Buzzonetti L, Rossetti L, Bertelli M. Mutation profile of BBS genes in patients with Bardet-Biedl syndrome: an Italian study. Ital J Pediatr 2019; 45:72-[PMID: 31196119].

11. Meng X, Long Y, Ren J, Wang G, Yin X, Li S. Ocular Characteristics of Patients With Bardet-Biedl Syndrome Caused by Pathogenic BBS Gene Variation in a Chinese Cohort. Front Cell Dev Biol 2021; 9:635216[PMID: 33777945].

12. Khan SA, Muhammad N, Khan MA, Kamal A, Rehman ZU, Khan S. Genetics of human Bardet-Biedl syndrome, an updates. Clin Genet 2016; 90:3-15. [PMID: 26762677].

13. Heon E, Kim G, Qin S, Garrison JE, Tavares E, Vincent A, Nuangchamnong N, Scott CA, Slusarski DC, Sheffield VC. Mutations in C8ORF37 cause Bardet Biedl syndrome (BBS21). Hum Mol Genet 2016; 25:2283-94. [PMID: 27008867].

14. Álvarez-Satta M, Castro-Sánchez S, Valverde D. Bardet-Biedl syndrome as a chaperonopathy: dissecting the major role of chaperonin-like BBS proteins (BBS6–BBS10–BBS12). Front Mol Biosci 2017; 4:55-[PMID: 28824921].

15. Melluso A, Secondulfo F, Capolongo G, Capasso G, Zacchia M. Bardet-Biedl syndrome: current perspectives and clinical outlook. Ther Clin Risk Manag 2023; 19:115-32. [PMID: 36741589].

16. Toms M, Pagarkar W, Moosajee M. Usher syndrome: clinical features, molecular genetics and advancing therapeutics. Ther Adv Ophthalmol 2020; 12:2515841420952194[PMID: 32995707].

17. Yoon CK. Syndromic Retinitis Pigmentosa. Inherited Retinal Disease: Springer; 2022. p. 99–108.

18. Castiglione A, Möller C. Usher Syndrome. Audiol Res 2022; 12:42-65. [PMID: 35076463].

19. Stiff HA, Sloan-Heggen CM, Ko A, Pfeifer WL, Kolbe DL, Nishimura CJ, Frees KL, Booth KT, Wang D, Weaver AE, Azaiez H, Kamholz J, Smith RJH, Drack AV. Is it Usher syndrome? Collaborative diagnosis and molecular genetics of patients with visual impairment and hearing loss. Ophthalmic Genet 2020; 41:151-8. [PMID: 32281467].

20. Mukherjee AB, Appu AP, Sadhukhan T, Casey S, Mondal A, Zhang Z, Bagh MB. Emerging new roles of the lysosome and neuronal ceroid lipofuscinoses. Mol Neurodegener 2019; 14:4-[PMID: 30651094].

21. Biswas A, Krishnan P, Amirabadi A, Blaser S, Mercimek-Andrews S, Shroff M. Expanding the neuroimaging phenotype of neuronal ceroid lipofuscinoses. AJNR Am J Neuroradiol 2020; 41:1930-6. [PMID: 32855186].

22. McArthur N, Rehm A, Shenker N, Richards A, McNinch A, Poulson A. Stickler syndrome in children: a radiological review. Clin Radiol 2018; 73:678-.

23. Robin NH, Moran RT, Ala-Kokko L. Stickler Syndrome Summary Genetic Counseling Suggestive Findings. Elsevier. 2021: 1–19.

24. Snead M, Martin H, Bale P, Shenker N, Baguley D, Alexander P, McNinch A, Poulson A. Therapeutic and diagnostic advances in Stickler syndrome. Ther Adv Rare Dis 2020; 1:2633004020978661[PMID: 37180493].

25. Mortier G. Stickler syndrome. GeneReviews®[Internet]: University of Washington, Seattle; 2023.

26. Boothe M, Morris R, Robin N. Stickler syndrome: a review of clinical manifestations and the genetics evaluation. J Pers Med 2020; 10:105-[PMID: 32867104].

27. Tehreem R, Chen I, Shah MR, Li Y, Khan MA, Afshan K, Chen R, Firasat S. Exome sequencing identified molecular determinants of retinal dystrophies in nine consanguineous Pakistani families. Genes (Basel) 2022; 13:1630-[PMID: 36140798].

28. Asghar A, Firasat S, Afshan K, Naz S. Association of CDKAL1 gene polymorphism (rs10946398) with gestational diabetes mellitus in Pakistani population. Mol Biol Rep 2023; 50:57-64. [PMID: 36301463].

29. Wang F, Wang Y, Zhang B, Zhao L, Lyubasyuk V, Wang K, Xu M, Li Y, Wu F, Wen C, Bernstein PS, Lin D, Zhu S, Wang H, Zhang K, Chen R. A missense mutation in HK1 leads to autosomal dominant retinitis pigmentosa. Invest Ophthalmol Vis Sci 2014; 55:7159-64. [PMID: 25316723].

30. Britten-Jones AC, Gocuk SA, Goh KL, Huq A, Edwards TL, Ayton LN. The diagnostic yield of next generation sequencing in inherited retinal diseases: a systematic review and meta-analysis. Am J Ophthalmol 2023; 249:57-73. [PMID: 36592879].

31. Botto C, Rucli M, Tekinsoy MD, Pulman J, Sahel J-A, Dalkara D. Early and late stage gene therapy interventions for inherited retinal degenerations. Prog Retin Eye Res 2022; 86:100975[PMID: 34058340].

32. Riaz M, Tiller J, Ajmal M, Azam M, Qamar R, Lacaze P. Implementation of public health genomics in Pakistan. Eur J Hum Genet 2019; 27:1485-92. [PMID: 31101884].

33. Dunbar CE, High KA, Joung JK, Kohn DB, Ozawa K, Sadelain M. Gene therapy comes of age. Science 2018; 359:eaan4672[PMID: 29326244].

34. Dai W-J, Zhu L-Y, Yan Z-Y, Xu Y, Wang Q-L, Lu X-J. CRISPR-Cas9 for in vivo gene therapy: Promise and hurdles. Mol Ther Nucleic Acids 2016; 5:e349[PMID: 28131272].

35. Banin E, Bandah-Rozenfeld D, Obolensky A, Cideciyan AV, Aleman TS, Marks-Ohana D, Sela M, Boye S, Sumaroka A, Roman AJ, Schwartz SB, Hauswirth WW, Jacobson SG, Hemo I, Sharon D. Molecular anthropology meets genetic medicine to treat blindness in the North African Jewish population: human gene therapy initiated in Israel. Hum Gene Ther 2010; 21:1749-57. [PMID: 20604683].

36. Shivanna M, Anand M, Chakrabarti S, Khanna H. Ocular ciliopathies: genetic and mechanistic insights into developing

therapies. Curr Med Chem 2019; 26:3120-31. [PMID: 30221600].

37. Méjécase C, Kozak I, Moosajee M, eds. The genetic landscape of inherited eye disorders in 74 consecutive families from the United Arab Emirates. American Journal of Medical Genetics Part C: Seminars in Medical Genetics; 2020: Wiley Online Library.

38. Khan MI, Azam M, Ajmal M, Collin RW, den Hollander AI, Cremers FP, Qamar R. The molecular basis of retinal dystrophies in pakistan. Genes (Basel) 2014; 5:176-95. [PMID: 24705292].

39. Ali A, Abdullah , Bilal M, Mis EK, Lakhani SA, Ahmad W, Ullah I. Sequence variants in different genes underlying Bardet-Biedl syndrome in four consanguineous families. Mol Biol Rep 2023; 50:9963-70. [PMID: 37897612].

40. Azam M, Khan MI, Gal A, Hussain A, Shah STA, Khan MS, Sadeque A, Bokhari H, Collin RW, Orth U, van Genderen MM, den Hollander AI, Cremers FP, Qamar R. A homozygous p.Glu150Lys mutation in the opsin gene of two Pakistani families with autosomal recessive retinitis pigmentosa. Mol Vis 2009; 15:2526-34. [PMID: 19960070].

41. Marwan M, Dawood M, Ullah M, Shah IU, Khan N, Hassan MT, Karam M, Rawlins LE, Baple EL, Crosby AH, Saleha S. Unravelling the genetic basis of retinal dystrophies in Pakistani consanguineous families. BMC Ophthalmol 2023; 23:205-[PMID: 37165311].

42. Kumaramanickavel G, Maw M, Denton MJ, John S, Srikumari CR, Orth U, Oehlmann R, Gal A. Missense rhodopsin mutation in a family with recessive RP. Nat Genet 1994; 8:10-1. [PMID: 7987385].

43. Lenassi E, Vincent A, Li Z, Saihan Z, Coffey AJ, Steele-Stallard HB, Moore AT, Steel KP, Luxon LM, Héon E, Bitner-Glindzicz M, Webster AR. A detailed clinical and molecular survey of subjects with nonsyndromic USH2A retinopathy reveals an allelic hierarchy of disease-causing variants. Eur J Hum Genet 2015; 23:1318-27. [PMID: 25649381].

44. Colombo L, Maltese PE, Castori M, El Shamieh S, Zeitz C, Audo I, Zulian A, Marinelli C, Benedetti S, Costantini A, Bressan S, Percio M, Ferri P, Abeshi A, Bertelli M, Rossetti L. Molecular epidemiology in 591 Italian probands with nonsyndromic retinitis pigmentosa and usher syndrome. Invest Ophthalmol Vis Sci 2021; 62:13-[PMID: 33576794].

45. Leijendeckers JM, Pennings RJ, Snik AF, Bosman AJ, Cremers CW. Audiometric characteristics of USH2a patients. Audiol Neurootol 2009; 14:223-31. [PMID: 19129697].

46. Jiang L, Liang X, Li Y, Wang J, Zaneveld JE, Wang H, Xu S, Wang K, Wang B, Chen R, Sui R. Comprehensive molecular diagnosis of 67 Chinese Usher syndrome probands: high rate of ethnicity specific mutations in Chinese USH patients. Orphanet J Rare Dis 2015; 10:110-[PMID: 26338283].

47. Dan H, Huang X, Xing Y, Shen Y. Application of targeted panel sequencing and whole exome sequencing for 76 Chinese families with retinitis pigmentosa. Mol Genet Genomic Med 2020; 8:e1131[PMID: 31960602].

48. Delmaghani S, El-Amraoui A. The genetic and phenotypic landscapes of Usher syndrome: from disease mechanisms to a new classification. Hum Genet 2022; 141:709-35. [PMID: 35353227].

49. Rao AR, Nazir A, Imtiaz S, Paracha SA, Waryah YM, Ujjan ID, Anwar I, Iqbal A, Santoni FA, Shah I, Gul K, Baig HMA, Waryah AM, Antonarakis SE, Ansar M. Delineating the spectrum of genetic variants associated with Bardet-Biedl syndrome in consanguineous Pakistani pedigrees. Genes (Basel) 2023; 14:404-[PMID: 36833331].

50. Abu Safieh L, Aldahmesh MA, Shamseldin H, Hashem M, Shaheen R, Alkuraya H, Al Hazzaa SA, Al-Rajhi A, Alkuraya FS. Clinical and molecular characterisation of Bardet-Biedl syndrome in consanguineous populations: the power of homozygosity mapping. J Med Genet 2010; 47:236-41. [PMID: 19858128].

51. Cárcel-Trullols J, Kovács AD, Pearce DA. Cell biology of the NCL proteins: what they do and don't do. Biochimica et Biophysica Acta (BBA)- Molecular Basis of Disease. 2015; 1852:2242-55. .

52. Azad B, Efthymiou S, Sultan T, Scala M, Alvi JR, Neuray C, Dominik N, Gul A, Houlden H. SYNaPS Study Group. Novel likely disease-causing CLN5 variants identified in Pakistani patients with neuronal ceroid lipofuscinosis. J Neurol Sci 2020; 414:116826[PMID: 32302805].

53. Lebrun AH, Storch S, Rüschendorf F, Schmiedt ML, Kyttälä A, Mole SE, Kitzmüller C, Saar K, Mewasingh LD, Boda V, Kohlschütter A, Ullrich K, Braulke T, Schulz A. Retention of lysosomal protein CLN5 in the endoplasmic reticulum causes neuronal ceroid lipofuscinosis in Asian sibship. Hum Mutat 2009; 30:E651-61. [PMID: 19309691].

Articles are provided courtesy of Emory University and The Abraham J. & Phyllis Katz Foundation. The print version of this article was created on 26 March 2025. This reflects all typographical corrections and errata to the article through that date. Details of any changes may be found in the online version of the article.